Journal of Volcanology and Geothermal Research 259 (2013) 373–388

Contents lists available at SciVerse ScienceDirect

Journal of Volcanology and Geothermal Research

journal homepage: www.elsevier.com/locate/jvolgeores

Volcano–ice interactions precursory to the 2009 eruption of Redoubt Volcano, Alaska

Heather A. Bleick [a,*], Michelle L. Coombs [b], Peter F. Cervelli [a], Katharine F. Bull [c], Rick L. Wessels [b]

[a] U.S. Geological Survey, Volcano Science Center, 345 Middlefield Rd., MS 910, Menlo Park, CA 94025, United States
[b] U.S. Geological Survey, Alaska Volcano Observatory, 4210 University Dr., Anchorage, AK 99508, United States
[c] Alaska State Division of Geological and Geophysical Surveys, Alaska Volcano Observatory, 3354 College Rd., Fairbanks, AK 99709, United States

ARTICLE INFO

Article history:
Received 3 June 2011
Accepted 15 October 2012
Available online 23 October 2012

Keywords:
Redoubt Volcano
Volcano–ice interaction
Precursory
Ice cauldron
Debris flow

ABSTRACT

In late summer of 2008, after nearly 20 years of quiescence, Redoubt Volcano began to show signs of abnormal heat flow in its summit crater. In the months that followed, the excess heat triggered melting and ablation of Redoubt's glaciers, beginning at the summit and propagating to lower elevations as the unrest accelerated. A variety of morphological changes were observed, including the creation of ice cauldrons, areas of wide-spread subsidence, punctures in the ice carved out by steam, and deposition from debris flows. In this paper, we use visual observations, satellite data, and a high resolution digital elevation model of the volcanic edifice to calculate ice loss at Redoubt as a function of time. Our aim is to establish from this time series a proxy for heat flow that can be compared to other data sets collected along the same time interval. Our study area consists of the Drift glacier, which flows from the summit crater down the volcano's north slope, and makes up about one quarter of Redoubt's total ice volume of ~4 km^3. The upper part of the Drift glacier covers the area of recent volcanism, making this part of ice mass most susceptible to the effect of volcanic heating. Moreover, melt water and other flows are channeled down the Drift glacier drainage by topography, leaving the remainder of Redoubt's ice mantle relatively unaffected. The rate of ice loss averaged around 0.1 m^3/s over the last four months of 2008, accelerated to over twenty times this value by February 2009, and peaked at greater than 22 m^3/s, just prior to the first major explosion on March 22, 2009. We estimate a cumulative ice loss over this period of about 35 million cubic meters (M m^3).

Published by Elsevier B.V.

1. Introduction

Redoubt Volcano is a 3110-meter-high stratovolcano in the Chigmit Mountains of the Aleutian Range in south-central Alaska, on the western side of Cook Inlet, about 180 km southwest of Anchorage (Figs. 1 and 2; see Bull and Buurman, 2013 for location map). Redoubt Volcano has erupted three times over the last 50 years: during 1966 through 1968, from December 1989 through June 1990, and, most recently, unrest activity from July 2008 through April of 2009. All of these reached a maximum volcanic explosivity index (VEI) of 3, involved explosive episodes intermixed with dome growth, produced mainly andesitic lavas and tephras, and disrupted a substantial fraction of the volcano's Drift glacier. Little else is known about the 1966–1968 eruption. The 1989–1990 eruption was, however, observed in detail, and because of the fortuitous installation of telemetered seismometers in the later summer of 1990, a nearly complete seismic record also exists. This eruption appeared to begin very suddenly, with little observed precursory activity. In contrast, the 2009 eruption was preceded by 8 months of episodic unrest that in its initial stages consisted mostly of changes in the summit glacier. The history of these changes, from their subtle beginnings to their catastrophic conclusion, is the focus of this paper. The large-scale lahars that inundated the Drift River valley due to explosive eruptions between March 22 and April 4, 2009, are described by Waythomas et al. (2012).

Retrospective analysis shows that the first indication of unrest appeared in July 2008, when observers noted areas of exposed rock at the top of both the 1966–1968 and 1990 lava domes. Both domes sit on the edge of the summit crater, which drains to the north through a steep-sided glacial valley that frames the upper Drift glacier (Fig. 1). The drainage continues down the Drift glacier and into the Drift River valley (Fig. 2). This region, bounded by the crater wall on the north, the lower Drift glacier on the south, and the flanks of the Drift glacier on the east and west, defines our study area.

2. Snow and glaciers

Because of its elevation and latitude, Redoubt receives ample precipitation, mainly in the form of snow, which sustains the volcano's glaciers. Trabant and Hawkins (1997) estimated Redoubt's total snow and ice volume at about 4.1 km^3 (Fig. 2). In comparison, this is about 34 times the volume of ice in the Crater Glacier at Mount St. Helens before its 2004–2006 unrest (0.12 km^3, of which 30% is estimated to be rock; Walder et al., 2008). Redoubt's snow and ice is roughly equivalent to the volume covering Mount Rainier, a higher and much more massive volcano in the Cascade Range southeast of Seattle, WA (Sisson et al.,

* Corresponding author. Tel.: +1 650 329 5261; fax: +1 650 329 5267.
E-mail address: hbleick@usgs.gov (H.A. Bleick).

0377-0273/$ – see front matter. Published by Elsevier B.V.
http://dx.doi.org/10.1016/j.jvolgeores.2012.10.008

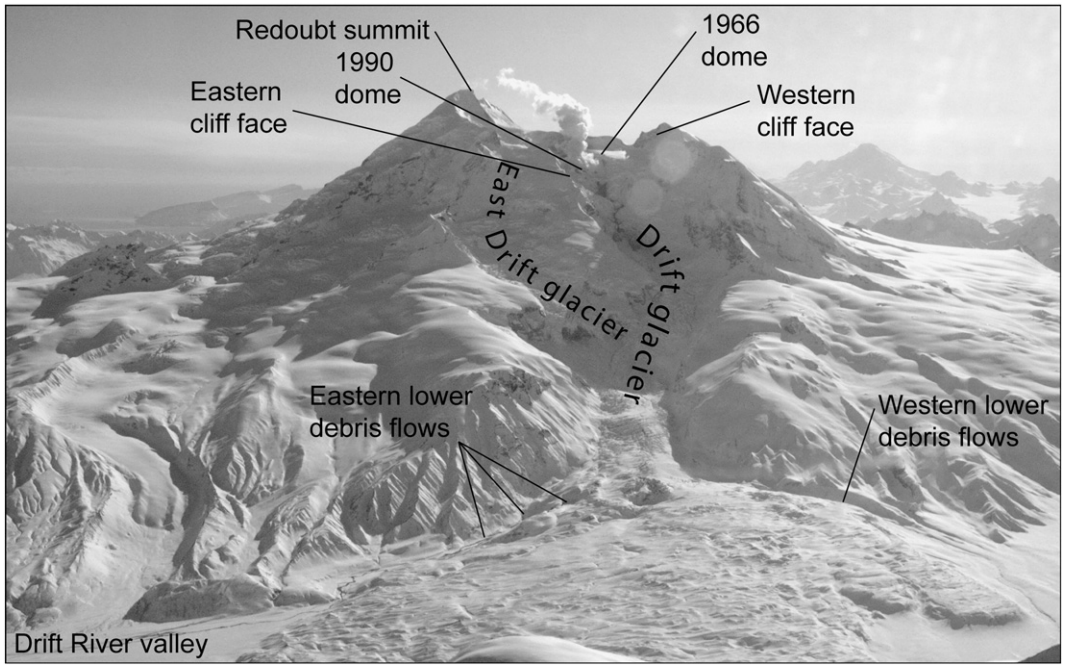

Fig. 1. North flank of Redoubt Volcano showing locations of key features.
Photo by H. Bleick AVO/USGS, taken March 15, 2009.

2011). The Drift glacier, which was informally named by Sturm et al. (1986), is the largest glacier on Redoubt, with a mean volume of about 0.98 $km^3 \pm 10\%$ (Trabant and Hawkins, 1997). Flowing north, the Drift glacier drains the 1.8 km wide summit crater through a breach at 2410 m ASL, and then flows down a steep valley with about 1750 m of relief over a distance of 6 km before it spreads into a spatula-shaped ice lobe about 3.5 km across (Fig. 2). The terminus altitude is about 300 m ASL, where the glacier reaches the Drift River. A single tributary glacier, which we call "East Drift glacier", descends from the summit crater through a gap to the east of the larger breach that feeds the Drift glacier (Fig. 2). The two meet at around 1000 m ASL. The Crescent glacier, which flows southwest from the summit ridge and drains into the North Fork of the Crescent River, is about 20% of the volume of the Drift glacier and the only other major glacier on Redoubt.

3. Observations and data

3.1. Features

The majority of features described in this paper are on the north flank of Redoubt Volcano, which had two domes prior to 2009, both at an elevation near 2500 m (Fig. 1). The western dome formed during the 1966 eruption (Miller, 1994) and its highest point projects through the summit ice-field, reaching an elevation of about 2530 m. The vent-clearing phase of the 1989–1990 eruption removed the eastern side of the 1966 dome. Between December 21, 1989 and mid-June, 1990, 14 distinct domes were emplaced in the same location east of the 1966 dome (Miller, 1994). Only the last dome remained, having an estimated volume of 10 M m^3. One of the first observed precursors to the 2009 eruption was the partial absence of snow and ice on both the 1966 and 1990 domes that was noted in July 2008. The exposed domes, considered unusual at the time, were almost certainly the earliest manifestation of an apparent increase in heat flux. Exposure of the lava domes was soon followed by progressively more dramatic phenomena, including ice-slurry flows, debris flows, holes in the ice, ice cauldrons, ejecta, crevasses, and a phreatic venting. Frequent satellite imagery and aerial photographs acquired throughout the eruption and unrest allowed us to track the disruptions over time, and ultimately led to important constraints of eruption parameters for the 2009 sequence (Figs. 3 and 4).

3.1.1. Definitions

The term "ice cauldron" describes a quasi-elliptical depression in the surface of a glacier caused by melting from heat applied at the basal interface (Björnsson, 1975, 1988; Gudmundsson, 2003; Gudmundsson et al., 2004). In general, the term ice cauldron covers a wide array of roughly circular subsidence features, ranging from shallow, uncrevassed depressions to deep, steep-sided, highly crevassed, nearly cylindrical voids (Gudmundsson et al., 2007). Ice cauldrons in Iceland tend to be several kilometers across and are usually much wider than they are deep, forming broad cone-shaped depressions (Gudmundsson et al., 2004). In contrast, the ice cauldron that formed in the summit crater of Redoubt Volcano, achieved a maximum width of 225 m and an estimated depth of about 100 m, with near-vertical walls (Figs. 3C and 5). This is similar in size to the initial depression that formed during the 1984 eruption of Veniaminof, Alaska (Yount et al., 1985). Various factors control the extent and style of subsidence, including the thickness of the ice roof, the melt rate, and the presence or absence of pre-existing fractures (crevasses). If the ice roof is thick (>100 m) or the melt (strain) rate is low, then ductile processes tend to predominate. In the alternative case, when the ice roof is thin (<100 m) or the melt rate high, brittle fracture occurs, creating arcuate roof cracks that roughly encircle the area of melt (Gudmundsson et al., 2007). Ice cauldrons can form during volcanic unrest that does not precede an eruption (e.g., Mount Spurr, Alaska, 2004–2006; Coombs et al., 2006).

In addition to ice cauldrons, we refer to other circular surficial features that formed from volcanically driven melting as "holes in the ice". Holes in the ice were typically tens of meters in width and formed above or near active fumaroles (Figs. 4A and 5B). They appear similar to what have been described as "ice chimneys" (Smellie, 2002 after Gudmundsson et al., 1997).

We also observe broad "subsidence areas", mostly near or within the summit crater (Fig. 6B). These subsidence areas were indistinct, did not expose bedrock, and changed more slowly than holes in the ice. However, their large size (approximately 600 m across) made them substantial contributors to the change in ice volume over the course the eruption.

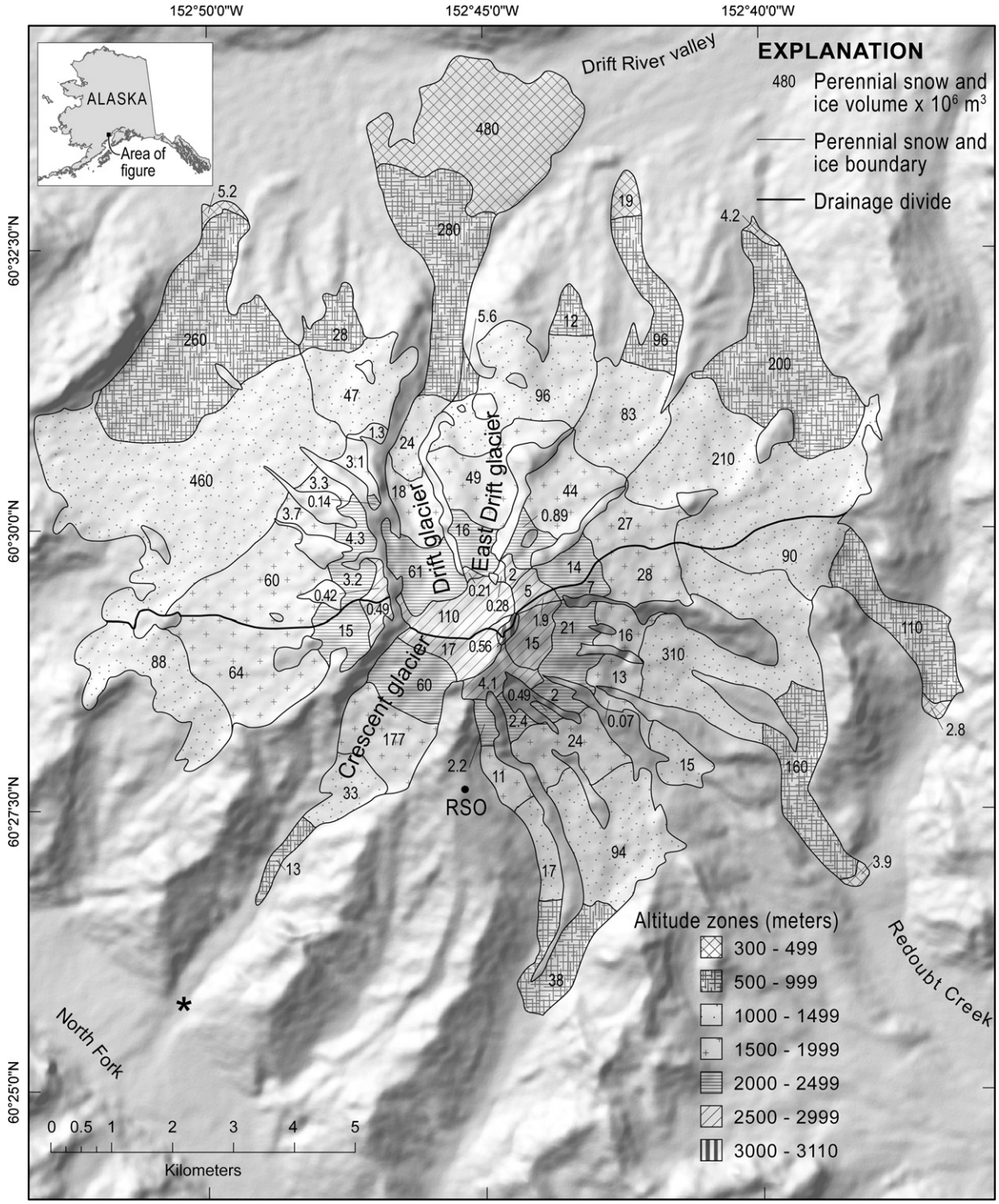

Fig. 2. Perennial snow and ice volumes arrayed by altitude sub-areas on Redoubt Volcano (modified from Trabant and Hawkins, 1997). Drainage divide separates the Drift River drainage to the north and the Crescent River drainage to the south.
Base image is hillside shading using DEM data from ASTER imagery taken October 20, 2008.

The general term "lahar", which describes mass flows composed primarily of volcaniclastic materials on a volcano, is not used here to describe the precursory flows leading up to the 2009 eruption. Instead, we use the term "debris flow" to define watery flows containing an unknown amount of water, sediment and ice chunks (Figs. 4B and 7). In previous eruptions, other terms to describe other types of flows have been used at Redoubt: jökulhlaup (Post and Mayo, 1971; Sturm et al., 1986), ice diamict (Gardner et al., 1994; Trabant et al., 1994; Waitt et al., 1994), mud flow (Post and Mayo, 1971), or avalanche of mixed snow and volcanic debris (Trabant et al., 1994).

In contrast to debris flow, we define an "ice-slurry" flow as the remains of a small sediment-poor ice or water flow, typically less than 400 m long, which can include varying amounts of loose snow in a slurry and flowing slush (Figs. 4E; Cronin et al., 1996; Thouret et al., 2007; Lube et al., 2009). The observed ice-slurry flows contained debris that was probably cobble-sized or smaller; larger particles were not

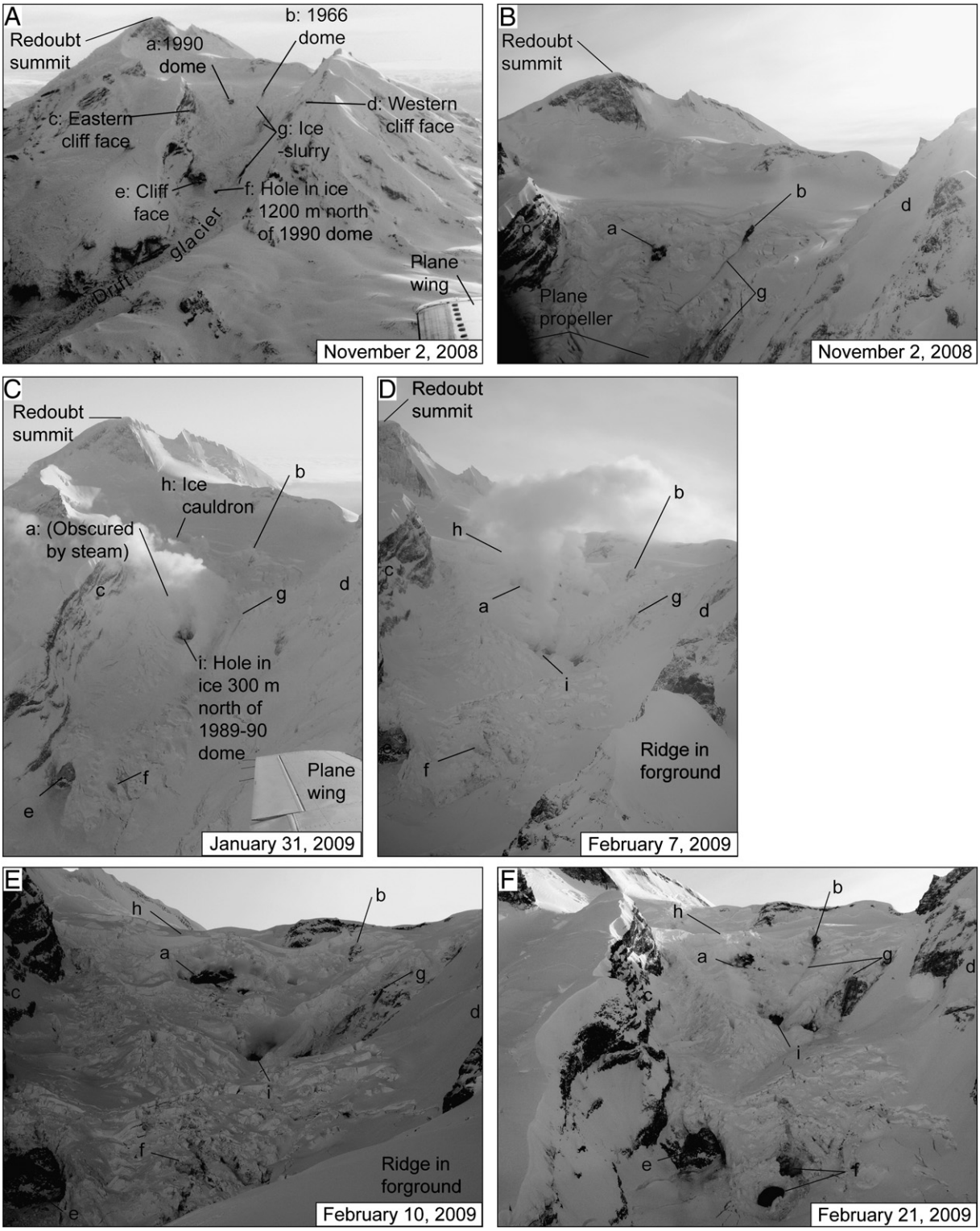

Fig. 3. Oblique aerial photographs of the north flank of Redoubt Volcano (looking south) showing features from November 2, 2008 through February 21, 2009. Labels 1990 dome and 1966 dome refer to the surface of the dome exposed through the glacier.
A and B) Photo by C. Reyes, AVO/UAF, November 2, 2008; C) Photo by R. Wessels, AVO/USGS, January 31, 2009; D) Photo by H. Bleick, AVO/USGS, February 7, 2009; E) Photo by G. McGimsey, AVO/USGS, February 10, 2009; F) Photo by G. McGimsey, AVO/USGS, February 21, 2009.

observed. However, all observations of these flows were made from the air, the deposits were not examined on the ground and no samples were collected.

A "burst deposit" is a radially directed sediment deposit that is on the order of tens of meters across, and is thought to consist primarily of granules or finer particles (Fig. 7C). However, because all observations were airborne, the deposits were never directly measured. Burst deposits were observed at the heads of debris flows that emerged at lower elevations on the Drift glacier, kilometers downslope from any known fumaroles, and in the absence of corresponding surficial flows

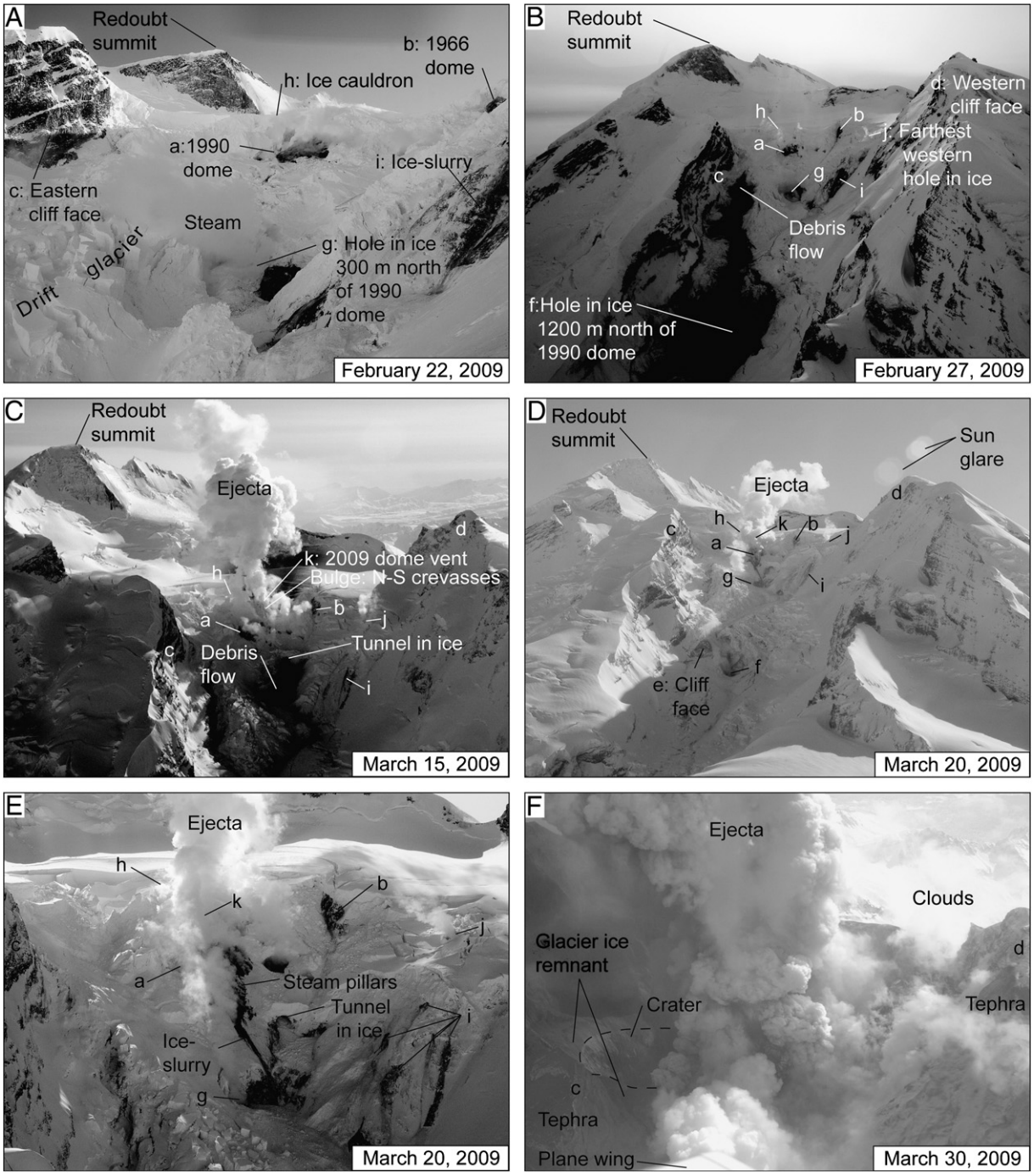

Fig. 4. Oblique aerial photographs of the north flank of Redoubt Volcano (looking south) showing features from February 22, 2009 through March 30, 2009. Labels 1990 dome and 1966 dome refer to the surface of the dome exposed through the glacier.
A) Photo by C. Read, AVO/USGS, February 22, 2009; B) Photo by C. Waythomas, AVO/USGS, February 27, 2009; C) Photo by H. Bleick, AVO/USGS, March 15, 2009; D) Photo by G. McGimsey, AVO/USGS, March 20, 2009; E) Photo by J. Schaefer, AVO/ADGGS, March 20, 2009; F) Photo by H. Bleick, AVO/USGS, March 30, 2009.

atop the upstream glacier. We observed several debris flows that we presume to have followed preexisting englacial (and possibly subglacial) pathways leading away and downslope from the summit basin. Burst deposits often occur where these pathways intersect crevasses or other weak points in the ice, as the mixture debouches onto the surface. We suggest that burst flows result from energetic flow within the englacial pathway caused by a surge in discharge.

Another depositional feature, coined a "spray deposit", occurs where an escarpment intersects a flow channel, forming from turbulent splashing and spraying at the bottom of the drop (Fig. 7B). Spray deposits range from 10 to 150 m across, scaling roughly with the escarpment height. Spray deposits rarely if ever leave marks, gouges, or tracks on the snow and ice, suggesting that they consist of granules or finer particles. No samples were available for direct measurements.

3.2. Chronology of ice-melt features

In this section we give a chronology of observations at Redoubt, beginning with the earliest signs of unrest in July 2008 up to the first major explosion on March 22, 2009 AKDT. Satellite data were acquired and

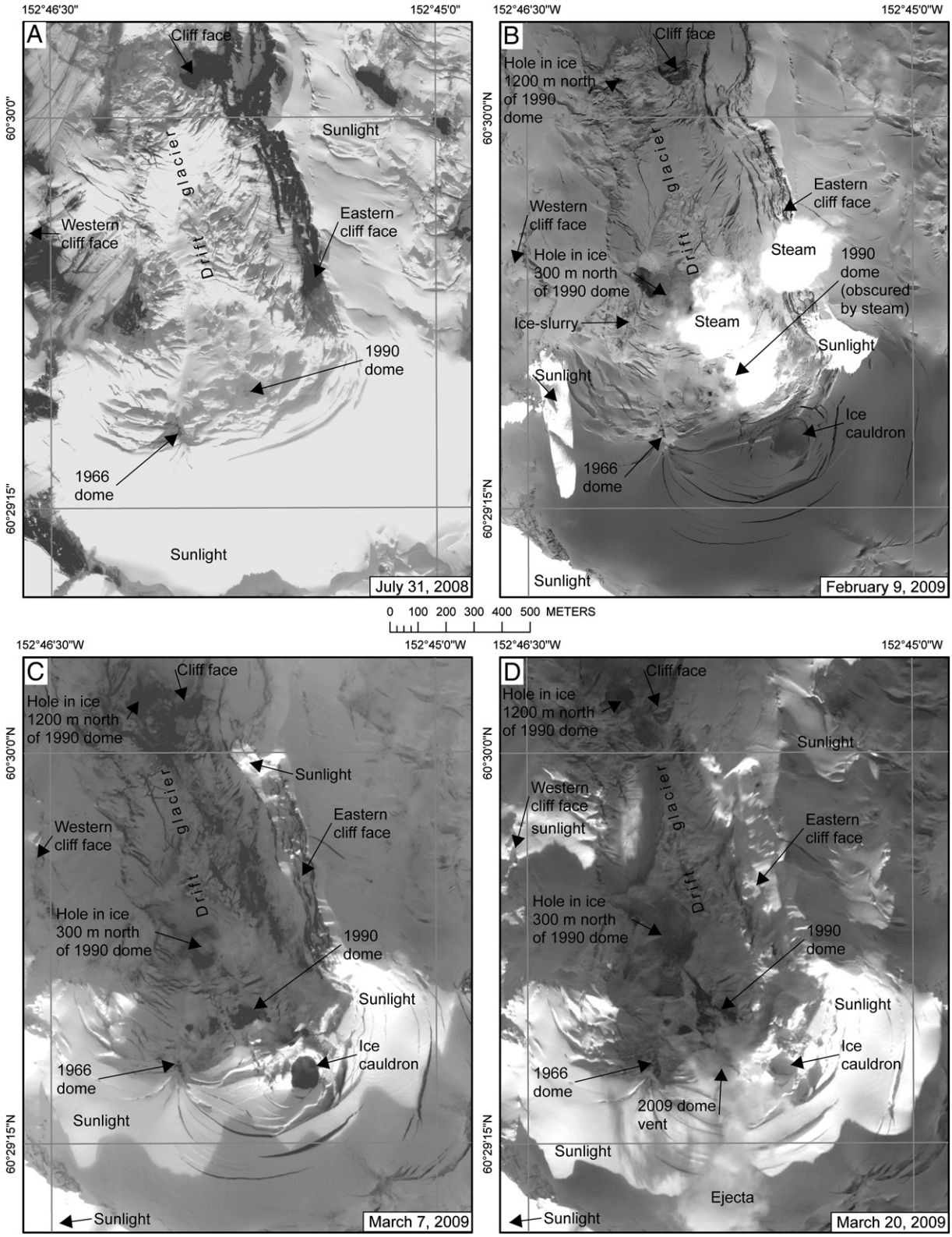

Fig. 5. Satellite images of the north flank of Redoubt Volcano, cropped and scaled to same area showing changes from July 31, 2008 through March 20, 2009. A) Image showing no obvious ice subsidence or cauldron. B) Image showing ice subsidence and ice cauldron. C) Image showing ice cauldron and exposed area of the 1990 dome. D) Image taken on March 20, 2009 showing areas of ice subsidence.

Panel A image from Quickbird (copyright DigitalGlobe, Inc.) taken on July 31, 2008 (image ID 052060236010). Panel B image from Quickbird (copyright DigitalGloabe, Inc.) taken on February 2, 2009 (image ID 052142263010). Panel C image from Quickbird (copyright DigitalGlobe, Inc.) taken on March 7, 2009 (image ID 052148999010). Panel D image from Quickbird (copyright DigitalGlobe, Inc.; image ID 052157258010).

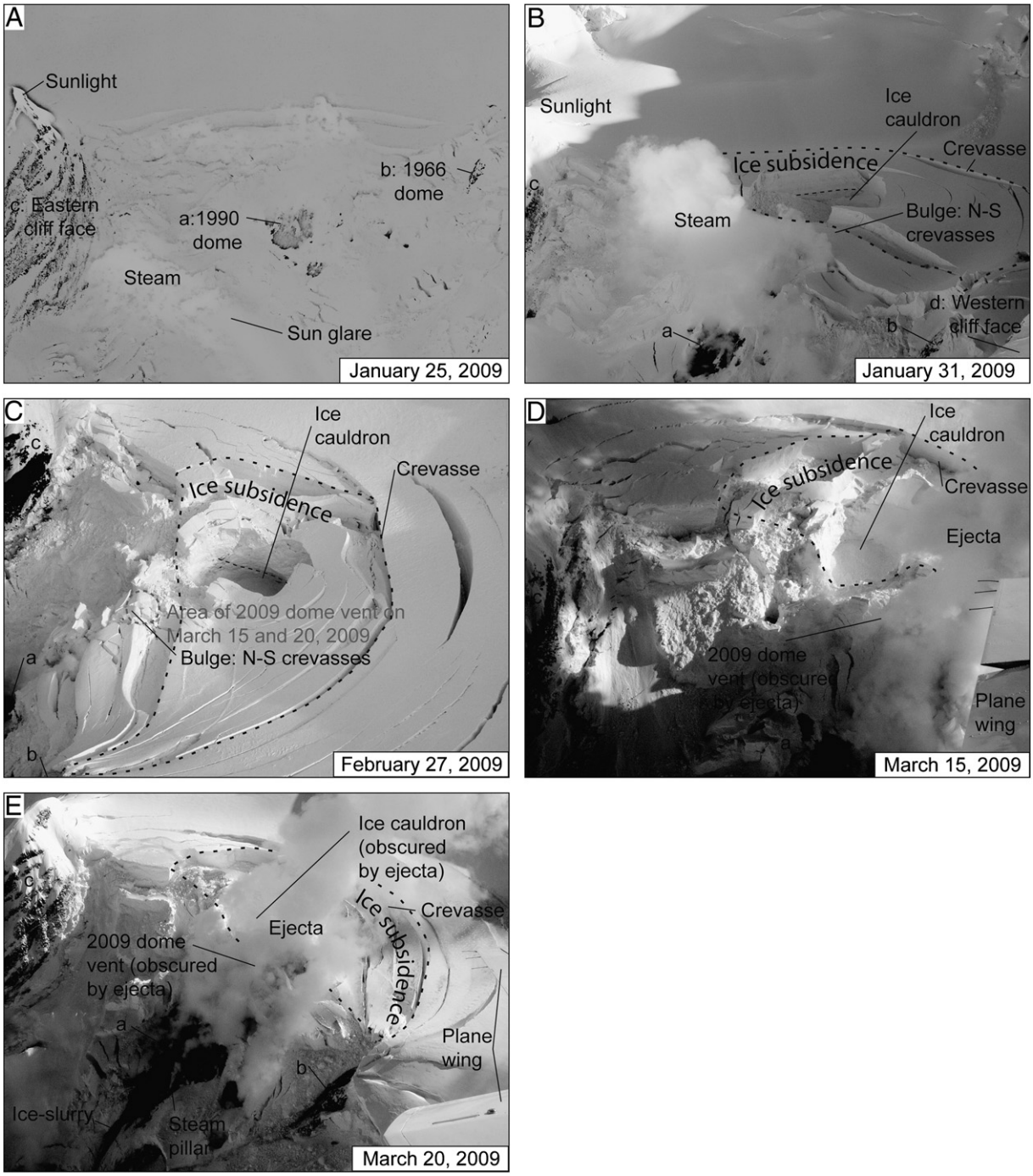

Fig. 6. Oblique aerial photographs of the ice cauldron in the summit crater on the north flank of Redoubt Volcano (looking south to east–southeast). Labels 1990 dome and 1966 dome refer to the surface of the dome exposed through the glacier.
A) Photo by H. Bleick, AVO/USGS, January 25, 2009 (looking south); B) Photo by T. Neal, AVO/USGS, January 31, 2009 (looking southeast); C) Photo by C. Waythomas, AVO/USGS, February 26, 2009 (looking east–southeast); D) Photo by H. Bleick, AVO/USGS, March 15, 2009 (looking southeast); and E) Photo by G. McGimsey, AVO/USGS, March 20, 2009 (looking southeast).

aerial photographs were taken frequently throughout this interval and provide us the means to track the evolution of various features as they appeared (Figs. 3, 4 and 5). A detailed description of the visual observations from July 2008 to March 22, 2009, is given in Appendix 1.

3.2.1. July through October 2008

The five main observations from the early precursory phase consist of: (1) a strong sulfur smell in the immediate vicinity of the volcano and also at times perceptible tens of kilometers away; (2) abnormally high spot temperature readings on the Drift glacier shown by Advanced Thermal Emission and Reflection Radiometer (ASTER) imagery; (3) visible melt features on the upper Drift glacier that were growing in size even as the season changed from summer to autumn (Fig. 5A); (4) a tremor-like seismic signal recorded on Redoubt's seismic network, coincident with loud explosion sounds, and a possible infrasonic pressure pulse recorded on instruments at nearby volcanoes (S. Stihler, written communication 2008); and (5) surficial debris flows exposed on the eastern side of the lower Drift glacier (Fig. 1).

Geologists working on the volcano in late July and early August 2008 reported smelling hydrogen sulfide (H_2S) near the edifice that varied in

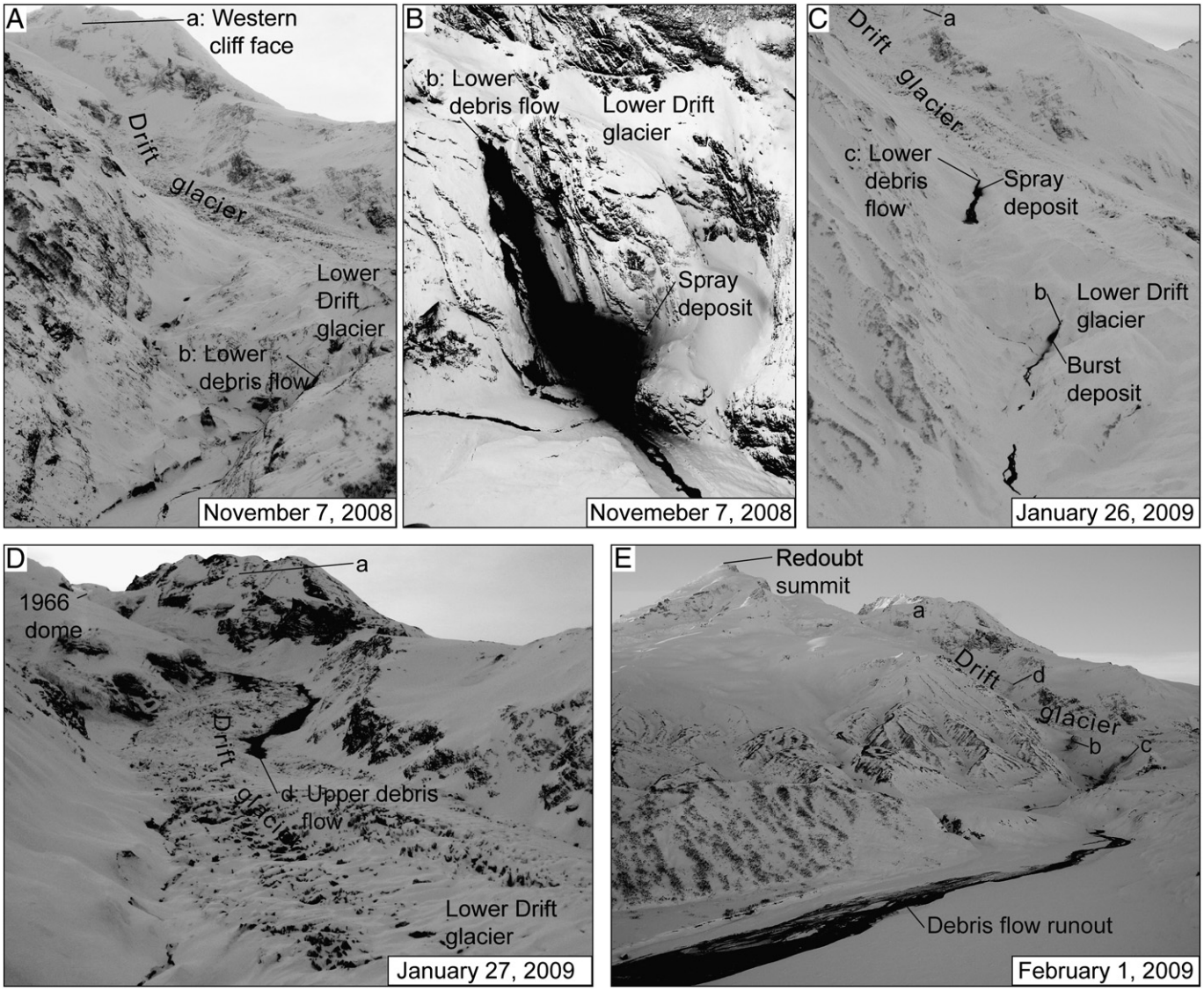

Fig. 7. Oblique aerial photographs of debris flows during the precursory phase of Redoubt Volcano 2009 eruption.
A) Photo by G. McGimsey, AVO/USGS, November 7, 2009 (looking southwest); B) Closer photograph of the debris flow labeled "b: Lower debris flow" showing a spray deposit. Photo by G. McGimsey, AVO/USGS, November 7, 2009 (looking west); C) Photo by T. Taylor, AVO/USGS, January 26, 2009 (looking southwest); D) Photo by R. Bierma, AVO/USGS, on January 27, 2009 (looking southwest). Label 1966 dome refers to the surface of the dome exposed through the glacier; and E) Photo by C. Read, AVO/USGS, February 1, 2009 (looking southwest).

intensity from imperceptible to "fairly" strong. At this time, only small areas of the 1966 and 1990 domes poked through the Drift glacier, and very few melt features had yet formed (Fig. 5A). Geophysicists from the Geophysical Institute of the University of Alaska Fairbanks conducted a GPS campaign from August 6 to 9, 2008. Comparison of photographs from the two parties reveal several new fumaroles formed above the 1990 dome sometime between late July and early August. Overflights to Redoubt on September 27 and October 13 revealed progressively more exposed rock over the 1990 dome area. On the September 27 flight, a circular 45–50-m-wide melt feature was observed on the upper Drift glacier about 1500 m north of the 1990 dome. The October 13 flight collected gas measurements of sulfur dioxide (SO_2; 30 tonnes/day, or t/d) and carbon dioxide (CO_2; 1370 t/d; Werner et al., 2013); the latter considerably above background. ASTER data from the same day shows two subtle thermal anomalies on the north flank of Redoubt Volcano, warmer than anything observed at the volcano over the prior eight years (Wessels et al., 2013-).

3.2.2. November through December 2008

An overflight on November 2 showed that most if not all of the existing melt features had enlarged and that many new features had formed (Fig. 3A). There were several ice-slurry flows and dozens of holes near the 1990 and 1966 domes, including a prominent hole in the Drift glacier, 1200 m north of the 1990 dome (Fig. 3A and B). Forward-Looking Infrared (FLIR) measurements on November 7 confirmed the increased temperatures first suggested by October's ASTER imagery.

Despite poor weather in late November and December 2008, a few observations were noteworthy. These include: (1) an apparent rock/ice fall or avalanche on November 11, which was detected by seismic instruments (S. Stihler, written communication 2008); (2) the widening and lengthening of crevasses on the rim of the summit crater south of the old domes; and (3) the persistence of fumaroles near the summit crater. Also in December 2008, a web camera was installed on "Ptarmigan ridge," about 11 km north of Redoubt Volcano summit, to observe the volcano's north flank.

3.2.3. January 2009

Bad weather continued through January and most satellite images showed nothing but clouds. Early on January 25, sustained volcanic tremor began that would wax and wane but remain nearly constant until the onset of the eruption in March (Buurman et al., 2013; Power et al., 2013). A small steam plume that reached an altitude of about 3100 m ASL was observed during an overflight later on January 25. Satellite data from this time show that the exposed area around the 1990 dome was larger than before, and four large holes in the ice were clearly visible between the 1990 and 1966 domes (Fig. 6A). A prominent hole in the ice 300 m north of the 1990 dome was the apparent source of the 3100 m steam plume. Within 24 h of the tremor onset, two debris flows occurred on the eastern margin of the lower Drift glacier (Fig. 7C). Run out flows appeared intermittently flowing into the tributary channel of Drift River and then disappeared under snow and ice. Several miles downstream the remains of the flow reappeared at the surface as murky water.

On January 26–27, additional, water-rich debris flows were observed flowing on top of the Drift glacier on the west side of the lower Drift glacier, leaving deposits 600–800 m long (Figs. 7D and 8A). These were the first flows observed to travel from the summit crater area over the Drift glacier.

On January 29, we first observed the ice cauldron and its large, encircling semi-circular crevasses in the summit crater near the 1990 dome (Figs. 3C and 6B). Its formation may have been correlated with elevated seismicity that started around 9:30 P.M. (AST) the day before and recorded several hour long periods of tremor (Buurman et al., 2013). With the formation of the ice cauldron, fumarolic features and pits near the summit crater were increasing in size and extent. By January 30, the ice surface between the 1990 and 1966 domes was irregular and crevassed. On January 31, there was a distinct sulfur odor as an overflight crew approached the volcano and the hole in the ice 300 m north of the 1990 dome jetted a vigorous plume (Fig. 3C).

3.2.4. February 2009

On February 2, the ice cauldron and circular crevasses in the summit crater were larger than the week before, and had apparently moved downslope to the north. Observations on February 7 showed that the majority of steam was emanating from two fumaroles: one near the upper part of the 1990 dome and the second from the hole in the ice 300 m north of the 1990 dome (Fig. 3D). The two plumes rose as distinct columns to 2500–2700 m ASL, and dissipated as they drifted south–southwest (Fig. 3D); repeat photos show possible pulses of stronger activity. CO_2 emissions on this day had roughly doubled from February 2 (Werner et al., 2013). On February 9 the Ptarmigan ridge web camera showed discrete puffing in the plume; the next day there was minimal steam observed (Figs. 3E and 5B).

FLIR images from February 10 showed a temperature of 1 °C on the 3–5-m-wide eastern debris flow, whereas the western debris flows appeared frozen (Wessels et al., 2013). The temperature of the exposed 1990 dome area had increased to 28 °C.

On February 17, the water-rich debris flows on the lower part of the Drift glacier appeared smaller and the western flow remained frozen at the surface. On February 21, the hole 1200 m north of the 1990 dome had significantly enlarged and steaming water poured into it (Fig. 3F). Drift glacier had fresh crack features that were not filled with snow and clean snow edges (Shad O'Neel, written communication 2009). Such features were not observed on the volcano's south side. On February 25, there was a broad-spectrum seismic signal beginning at 9:29 A.M. and the next web camera image at 10:03 A.M. showed a new 300-m-long debris flow just below the large hole in the ice 1200 m north of the 1990 dome.

Starting at 5:30 P.M. February 26, the number of shallow earthquakes increased and remained elevated for about an hour. These events were accompanied by the emplacement of a debris flow, visible beginning at 6:04 P.M. on the web camera images. An ASTER thermal infrared satellite image from the evening of February 26 showed

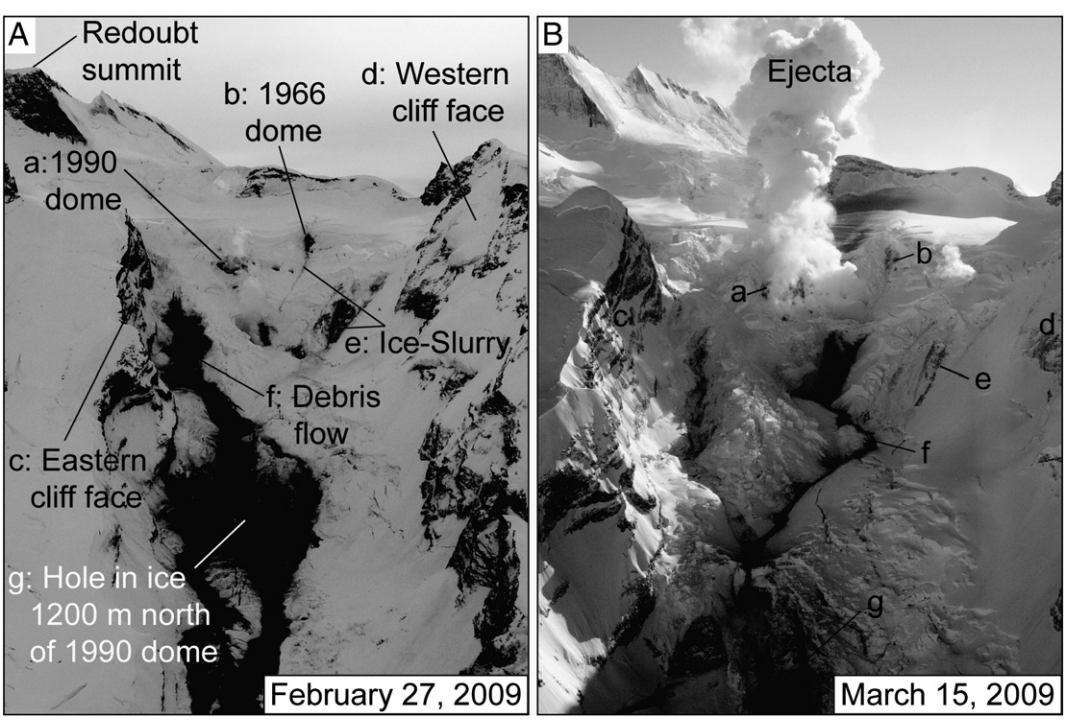

Fig. 8. Oblique aerial photographs of debris flows on the upper region of the north flank on Redoubt Volcano (looking south to east–southeast). Labels 1990 dome and 1966 dome refers to the surface of the dome exposed through the glacier.
A) Photo by C. Waythomas, AVO/USGS, February 27, 2009 (looking south) and B) Photo by H. Bleick, AVO/USGS, March 15, 2009 (looking south).

this warm (39–63 °C) area stretching several kilometers down the Drift glacier (Wessels et al., 2013).

On February 27 there was an obvious debris flow on the surface of Drift glacier, thick enough in most places to obscure the underlying snow/ice (Figs. 4B and 8A). The debris was deposited on February 26 and most likely continued into February 27. The flow appeared to originate from a hole in the ice just downslope and slightly east of the 1990 dome. It extended to about 1000 m and did not appear to transform to a more watery flow beyond its terminus. Also on this day we noted considerably more subsidence of the ice near the 1990 dome, including the ice cauldron, which appeared to have foundered and become fractured and broken (Fig. 6C). ASTER TIR imagery showed elevated temperatures for the ice cauldron (56 °C), the 1990 dome area (37 °C), the hole in ice 300 m north of the 1990 dome (69 °C), and the hole in ice 1200 m north of the 1990 dome (15–90 °C; Wessels et al., 2013).

3.2.5. March 2009

Changes to the ice features were minor in early March, but increased rapidly leading up to the eruption in mid-March. There were no obvious new features observed in satellite imagery from March 1 to 12 (Fig. 5C). Fresh snow obscured the debris flows from late February. The level of steam emissions decreased and seismicity declined. However, melting of the Drift glacier in the vicinity of the 1990 dome continued (Fig. 9).

During a gas and observational overflight on March 15, seismicity increased noticeably at about 1:05 P.M., accompanied by increased steaming and the highest CO_2 and SO_2 measurements seen to date (Werner et al., 2013). A small phreatic explosion resulted in a plume that rose to 3700–4000 m ASL, and was notably darker and more voluminous than any other plume observed thus far (Fig. 4C). The vent for this activity was located tens of meters south of the exposed 1990 dome and was approximately 100 m in diameter (Figs. 4C and 6D). A dusting of tephra was limited to the south crater floor, rim, and extending south–southeast perhaps 6 to 8 km, roughly covering an area of 2.8 M m^2.

About 20 min after the phreatic explosion, an outflow of debris occurred from a tunnel above the hole in the ice 300 m north of the 1990 dome (Schaefer, 2012; Wallace et al., 2013; Fig. 4C and E). This burst discolored the ice headwall and produced a debris flow that filled the hole in the ice 300 m north of the 1990 dome and then descended 500 m (Fig. 8B). Continued discharge from this area enlarged the extent of the debris flow downslope, and by 3:40 P.M. the flow extended to 1200 m in length. Debris-rich water cascaded over bedrock forming a waterfall that disappeared into a hole in the ice about 1200 m north of the 1990 dome.

Vigorous vapor emissions during the phreatic explosion came from the 1990 dome surface, holes west of the 1990 dome and the hole in the ice 300 m north of the 1990 dome. There were also vigorous emissions visible from the area west of the 1966 dome (labeled "j: farthest western hole in ice" in Fig. 4). This overall increase in vigor coincided with an SO_2 emission rate measured at 3850 t/d, which was roughly 40 times higher than previous measurements (Werner et al., 2013).

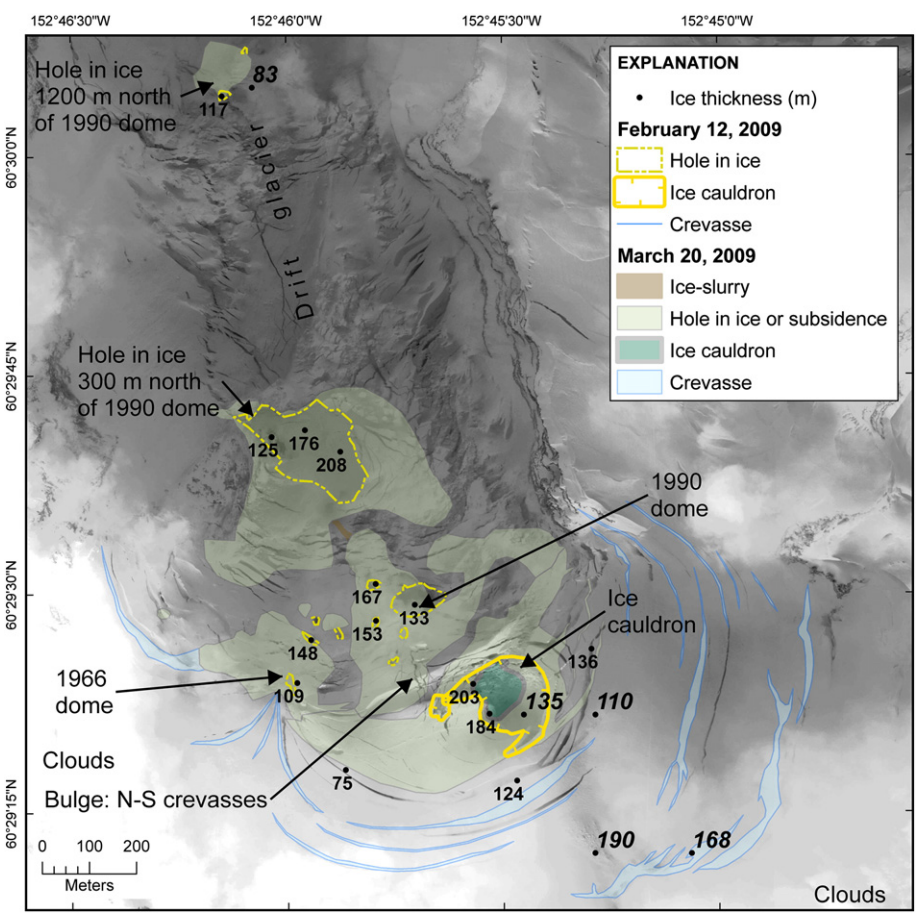

Fig. 9. Comparing features observed on February 12, 2009 and March 20, 2009 with satellite image of the north flank of Redoubt Volcano taken on February 12, 2009. Ice thickness points are calculated values described in text.
Bold-italic ice thickness values are from Trabant and Hawkins, 1997. Image from Quickbird (copyright DigitalGlobe, Inc.; image ID 052142262010).

The first magmatic explosions on March 22 were preceded by approximately 58 h of elevated broad spectrum seismicity (Power et al., 2013). Eruption columns reached 18,300 m (60,000 ft) with the bulk of the ash between 7600 and 9100 m (25,000–30,000 ft) (Schneider and Hoblitt, 2013). Lahars accompanied the largest of these explosions. The head of the lahar was down the center of the Drift glacier, where it formed a deep gorge in the ice as it flowed further downstream and across the glacier. From this point, the lahar inundated 35 km of the Drift River Valley reaching the Cook Inlet with high-water marks up to 6 to 8 m above the channel floor and depositing car-sized blocks of glacial ice. For further descriptions of the lahars associated with the eruption after March 22, 2009, see Waythomas et al. (2012).

4. Ice loss

4.1. Method

To estimate the volume of melted ice as a function of time from the first signs of unrest through the beginning of the eruption, we examined all relevant imagery looking for the various kinds of melt features, and then approximated the volume of the void space to estimate ice loss. We paid particular attention to ice cauldrons, crevasses, holes in ice associated with fumaroles, ice subsidence areas, and debris flows. Debris flows help constrain the timing of melt events, and can serve as directional indicators pointing back toward a source area, but otherwise do not contribute to our melt history analysis.

Calculating the volume of void space left after melting occurred requires knowledge of the dimensions and shape of the void. We represented each void as a vertical prism with faces defined by the traced perimeter of the melt feature and height equal to ice depth. Voids with shapes that could not be easily represented as a single prism were broken down into sub-voids, which were assigned separate perimeter and depth measurements. The total volume estimate was the sum of all the sub-voids.

We traced the perimeters of melt features on orthorectified satellite images and/or photos from observation flights, using ArcGIS software, usually limited by the resolution of the base image and look angle (Figs. 5, 9 and 10). The vertical dimensions of melt features were more difficult to measure and constitute a major source of uncertainty in the overall calculation. In cases where the voids reached down to bedrock, we used ice thickness as the void height, but even in these cases, the slopes of the void walls were largely unknown.

Determining the depth of a void requires knowledge of the local ice thickness. Trabant and Hawkins (1997) provided a catalog of ice thickness throughout the Redoubt area, but recent direct measurements on the Drift glacier were few. To estimate overall ice thickness on the glacier, we compared bare ground elevation data to elevation data that include the ice. Bare ground topography was measured from aerial photography in 1990, after the 1989–1990 eruption had scoured away much of the Upper Drift glacier, and later converted to a digital elevation model (DEM). The majority of the DEM represents ice-free ground, but a few areas in the summit crater and the bases of some ravines still retained some ice. ASTER satellite images, collected in October 2008, were used to derive a DEM of ice-covered Redoubt. By differencing the 1990 and 2008 DEMs, we obtain a model of ice thickness. At best we estimate error for our ice-thickness values to be $\pm 30\%$. This is largely due to 30 m pixel size and variable vertical resolution for ASTER data. Additionally, the 1990 DEM had ice cover in parts, which would make the ice thickness values be minimums. We checked our model by comparing the calculated thicknesses to those point values given by Trabant and Hawkins (1997).

Trabant and Hawkins (1997) measured 46 sites on Redoubt Volcano in August 1989 using a surface-based monopulse ice-radar system (Fig. 9). Only five glacier thickness measurements are on the upper part of the Drift glacier near the majority of the 2009 ice loss features (Fig. 9). Four out of the five sites are in the summit crater and yield thicknesses of 110, 135, 168, and 190 m. Our calculated values for this area in the summit crater are similar ranging from 75 to 203 m. At another location, at the hole in the ice 1200 m north of the 1990 dome, our calculated value of 152 m corresponds only fairly well with previous calculated values of Trabant and Hawkins (1997) at 83 m. The ice was generally thicker at the northern edge of the crater summit, and thinnest near the 1966 dome and at the hole in the ice 1200 m north of the 1990 dome.

4.2. Results

Table 1 and Appendix 2 show ice loss in millions of cubic meters (M m^3) as a function of time from July 2008 through March 2009. The rate of ice loss was comparatively slow during the early precursory stage of the eruption, averaging about 0.1 m^3/s until October 2008. After this, the rate doubled to about 0.2 m^3/s, melting nearly 2.5 M m^3 of ice by January 25, 2009. At this time, the melt rate rose by more than an order of magnitude to 2.2 m^3/s, resulting in a cumulative ice loss of around 5 M m^3 by February 12 (Fig. 9). By early March, the cumulative ice loss surpassed 10 M m^3, reaching a rate of 4.1 m^3/s. In mid-March, the ice loss rate jumped to about 22 m^3/s, resulting in more than 35 M m^3 of melt by the start of the eruption on March 22, 2009.

The main contributor to the ice loss during the 6 day interval from January 25 through January 31, 2009, was the formation of the upper ice cauldron within the summit crater (Fig. 6). Using satellite imagery, we calculate the area of the ice cauldron to have been about 17,000 m^2, and estimate the approximate depth at 40 m (the total ice thickness in this area is about 180 m). This result is an ice cauldron volume of about 680,000 m^3 (Appendix 2). Over the next 3 days, most of the ice loss came from the enlargement of the hole in the ice 300 m north of the 1990 dome (Figs. 3 and 4). Close examination shows the existence of two distinct holes in this area, an eastern and a western, with the former being about 10 times smaller than the latter (Fig. 4A). The western hole bottomed out at bedrock in ice that was 170 m thick and had an area of about 21,000 m^2. The shape of the western hole was not a simple cylinder—it looked more like a bowl with deep depression in its center (Fig. 4A). While calculating the volume of the western hole, we accounted for the irregularity, yielding a corrected volume of about 2.4 M m^3. By February 24, 2009, the ice cauldron had doubled in volume to about 1.4 M m^3, and the western hole had enlarged to more than 3.6 M m^3. Curiously, as the ice cauldron grew in volume, its area shrank, though rate of deepening more than offset this effect on its volume (Figs. 9 and 10).

Approximately 4% of the volume of the Drift glacier had melted by the time the first phreatic explosive event occurred on March 15, 2009. In late March, 2009, the top of the East Drift glacier was also affected by the eruption, creating a mass flow consisting of ice, snow, and some water.

4.3. Water and gas chemistry and thermal trends

Over the precursory stage of the eruption, Alaska Volcano Observatory (AVO) scientists collected several water samples along the eastern margin of the lower Drift glacier near the debris flow shown in Fig. 7B (WGS84 coordinates N60°32′50.0″, W152°44′21.4″). While sampling at this site on February 10, 2009, G. McGimsey observed a doubling of discharge rate, during which the flow changed to about 50% ice and the temperature of the water dropped from 1.5 °C to 0.4 °C, possibly caused from upstream release of an ice conduit. Analysis showed that the water sample from this site was high in Mg and Fe, but low in SiO_2, a combination indicative of consistently low temperatures (Werner et al., 2012).

Our estimates for cumulative ice melt correlate well with the cumulative SO_2 and CO_2 gas flux release from Redoubt over the course of the precursory stage of the eruption (Fig. 10B; Werner et al., 2012).

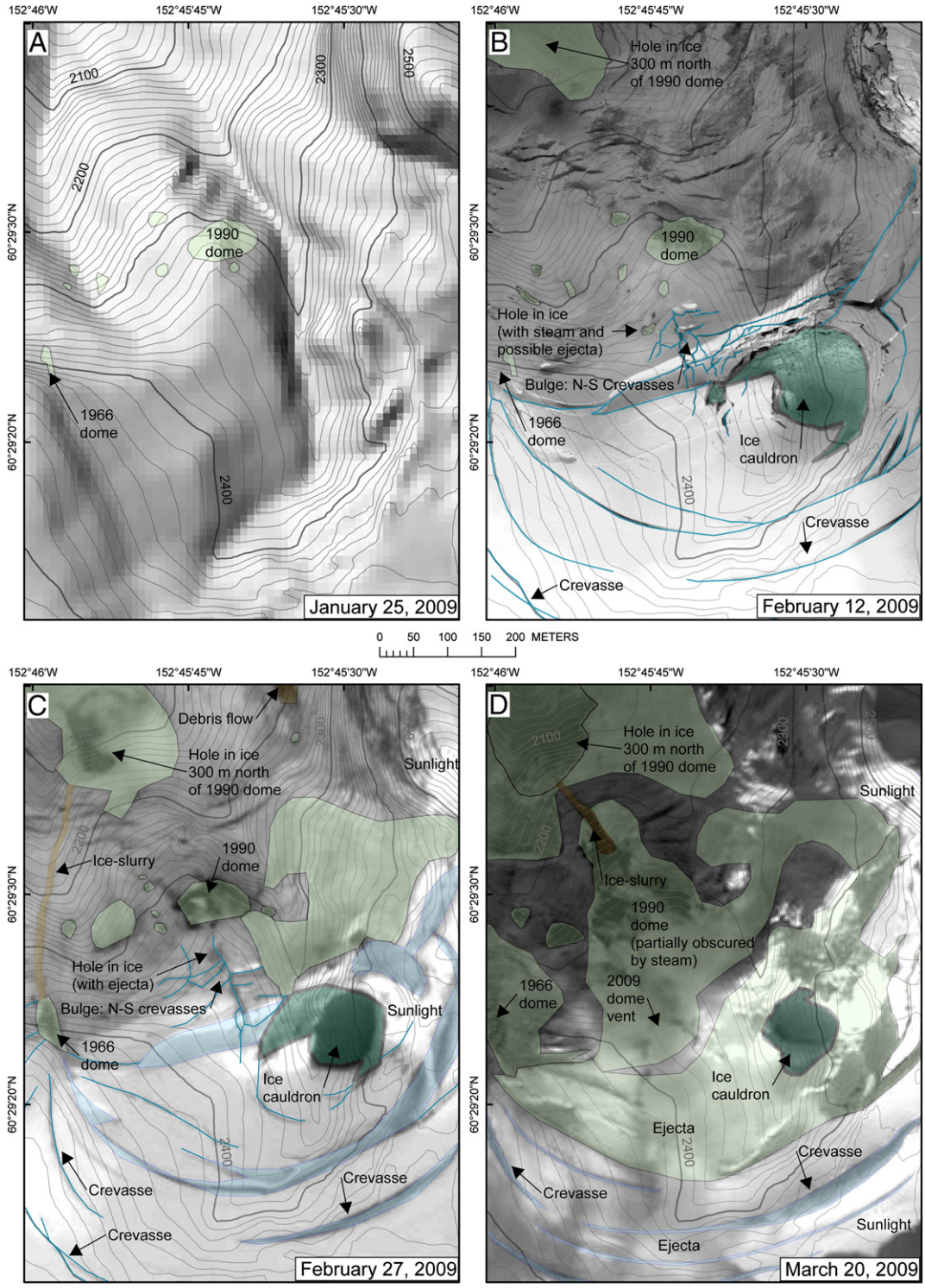

Fig. 10. Images of the summit crater area. Key: dark green—ice cauldron; light green—hole in ice or subsidence; blue—crevasses; brown—ice-slurry flow. Contour lines are from the 1990 topographic map. A) Features observed on January 25, 2009, shown on the digital elevation data from 1990 topographic map. B) Features observed on February 12, 2009, shown overlying satellite image from Quickbird (copyright DigitalGlobe, Inc.) taken on February 12, 2009 (image ID 052142262010). C) Features observed on February 27, 2009, shown overlying satellite image from Quickbird (copyright DigitalGlobe, Inc.) taken on February 27, 2009 (image ID 052149001010). D) Features observed on March 20, 2009, shown overlying satellite image from Quickbird (copyright DigitalGlobe, Inc.) taken on March 20, 2009 (image ID 052157258010).

Likewise, thermal measurements from both FLIR and the ASTER satellite show a similar pattern of temperature increase during this interval (Wessels et al., 2013). The correlation with these two independent data sets is consistent with rising magma underneath the volcano in the months preceding the eruption in March.

Gas measurements taken on March 15 showed a large increase in SO_2 flux, coinciding with jump in melt rate we observed at this time (Fig. 10). Werner et al. (2012) suggest that by this stage in the unrest, magma was freely degassing from a mid-crustal depth. Prior to this date, the lack of abundant SO_2 suggests a deeper magma that was not

Table 1
Estimate ice loss during precursory phase of 2008–2009 eruption of Redoubt Volcano.

Date	Cumulative ice loss (m^3)	Percent ice loss of Drift glacier	Days elapsed	Ice loss per second (m^3/s)	Ice loss per second by groups (m^3/s)	Heat transfer rate melting ice (MW)	Heat transfer rate melting ice by group (MW)	Comments on increase of ice loss
July 31, 2008	95,257	0.01	0	–	–	–	–	
October 2, 2008	420,765	0.04	63	0.1	0.1	19	19	
November 2, 2008	769,299	0.08	31	0.1	–	40		
January 25, 2009	947,897	0.09	84	0.0	–	8		
January 31, 2009	2,425,583	0.24	6	2.9	0.2	876	59	Ice cauldron formed in summit crater
February 2, 2009	4,242,806	0.42	2	10.5	–	3238		Hole in ice 300 m north of 1990 dome enlarges
February 9, 2009	4,531,316	0.45	7	0.5	–	147		
February 12, 2009	4,754,175	0.48	3	0.9	–	237		Hole in ice 300 m north of 1990 dome enlarges
February 24, 2009	6,909,195	0.69	12	2.1	2.2	647	670	
March 1, 2009	9,040,937	0.90	5	4.9	–	1552		Large area around the 1990 dome subsidence
March 7, 2009	10,805,710	1.08	6	3.4	4.1	1081	1300	
March 18, 2009	26,819,507	2.68	11	16.8	–	4866		Phreatic explosion on March 15, 2009
March 20, 2009	36,158,792	3.62	2	54.0	22.6	18,060	6900	Large ice subsidence area around the 1990 dome area and 300 m north of 1990 dome

free to degas. Our melt rate estimates confirm the interpretation, and the combination of both data sets strongly implies that magma was nearing the surface by mid-March 2009.

5. Discussion

5.1. Features: upper ice cauldron, bulge, steam pillars, and features on the East Drift and Crescent glaciers

5.1.1. Upper ice cauldron

Interesting questions surround the development and evolution of the summit ice cauldron. The cauldron formed at about 2422 m ASL in the upper part of a 200 m wide small drainage that feeds northward through a breech in the summit crater at about 2400 m ASL (Fig. 10A). We suggest that the ice cauldron resulted from subglacial geothermal heating. Melt water resulting from such activity can accumulate or continuously drain (Gudmundsson et al., 2007). We propose that in this case, melt water accumulated as a subglacial lake, and that the roof of the cavity above the lake began to sag and collapse to form the surface expression of the ice cauldron. This has been documented at Mount Spurr, Alaska, in 2005 by Coombs et al. (2006). In such lakes, cracks in the glacier or basal channels or permeable layers in the ice or in the underlying sediment or bedrock, facilitate the release of water at hydrostatic pressures less than those required to "float" the surrounding ice (Fisher, 1973; Nye, 1976; Björnsson et al., 2003). This is likely true at Redoubt Volcano as well, although water was not observed in the summit crater.

We suggest that the size of the subglacial lake can be inferred from the extent of the arcuate crevasses that surrounded the ice cauldron (Figs. 6 and 10). Because both the ice cauldron and the arcuate crevasses formed on the same day, we suggest that both features are the result of collapse into the same cavity, the area of which was about 0.14 km^2 (Fig. 6). If the arcuate crevasses are taken to show the approximate boundaries of the lake, then the area is about 10–15% smaller; however it is plausible that the lake's eastern boundary was coincident with the eastern cliff, since this is where the start of the debris flow occurred on February 27 (Figs. 8A and 10). The existence of this subglacial lake could explain the source of the water for the February 27 debris flow on top of the Drift glacier (Fig. 8A). We hypothesize that the lake was contained until this date, presumably with some kind of ice dam or melting conditions may have been higher than discharge via cracks and basal channels away from the summit crater area, creating ponding of water. Eventually, the lake breached at around 2420 m ASL (Fig. 10A), drained down the eastern side of Drift glacier, and finally debouched as a debris flow from a small hole in the ice on the east side of the valley at around 2250 m ASL (Fig. 10C).

As noted above, the areal extent of the ice cauldron was observed to decrease over time, though the volume continued to increase as the cauldron deepened (Figs. 9 and 10). We suggest that this apparent change in area occurred for two reasons: (1) glacial flow during the observation interval distorted the shape of the ice cauldron, and (2) the debris flow of February 27, 2009 drained enough of the subglacial lake that the plug ice in the cauldron above the lake dropped almost to bedrock thus stabilizing the whole area under collapse.

5.1.2. Bulge

An interesting feature seen in high-resolution satellite images was a crevasse system trending north–south above the vent for the March 15 phreatic explosion and near the first vent of the 2009 dome exposed at the surface on March 20 (Figs. 6C, 9 and 10B and C). North–south crevasses are rare in the Drift Glacier. Most are east–west, perpendicular to the flow down the valley. This fracture system was small, approximately 150 m north–south × 100 m east–west with crevasses estimated to be less than 15 m in width, and was first seen on images from January 31, 2009. The fracture system was not above a bedrock low, but rather, directly above the 1990 dome as seen in the bare earth DEM (Fig. 10). We present the possibility of localized ground deformation of bedrock at the site of the 1990 dome as the cause of the north–south fracture system in the glacier. The fracture system appears as a bulge (Walder et al., 2008) in the glacier from late January until the eruptions in mid-late March. The February 12 imagery reveals a small hole in the ice (20 × 10 m) near the bulge with a trace of ejecta around the hole (Fig. 10B). It is presumed this material is phreatic. We do not see evidence of flowing water but steam is visible. On the February 27 image there is another hole near the north–south fracture system (Fig. 10C). And on March 15, a larger hole was formed near the fracture system that produced the phreatic ejecta (Fig. 10D). Emission from the new vent appeared vigorous and pressurized.

5.1.3. Steam pillars

We define a steam pillar as a chimney of steam and gas less than several meters wide. The column of a steam pillar is tens of times longer than it is wide and appears funnel shaped being more narrow at the base in a tight column. They often form in groups. As steam from the pillars rise approximately 100 m or more, the discrete column appears to become disaggregated as it becoming broader and wider. It then is indistinguishable with the steam plume seen in the overall larger area.

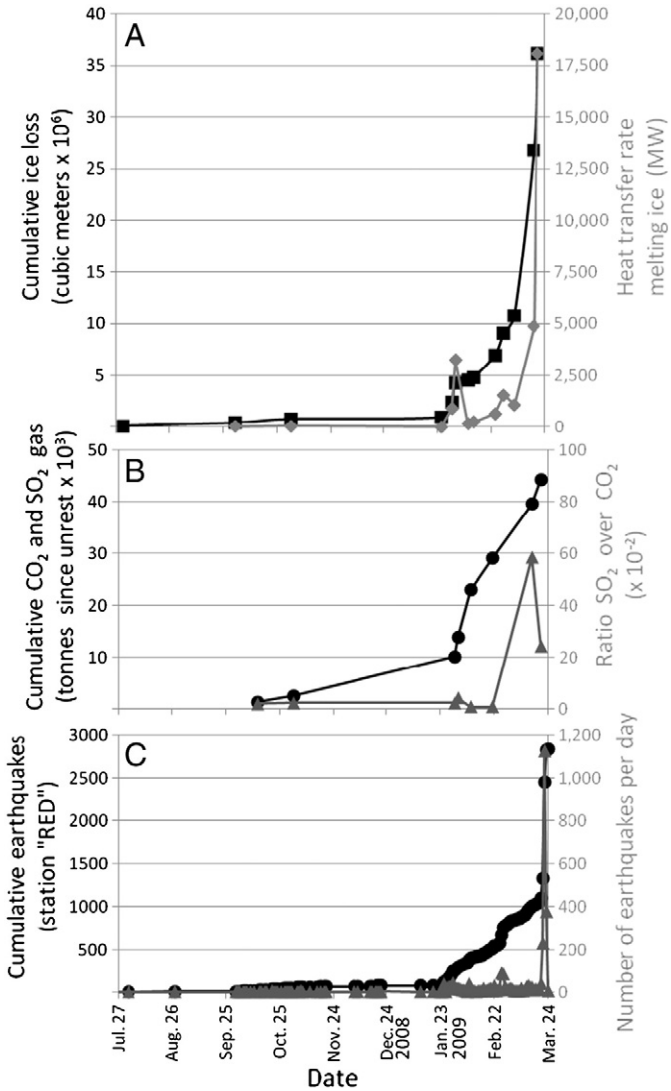

Fig. 11. Correlation between ice loss, gas flux, and seismicity for Redoubt Volcano 2008–2009 eruption. A) Estimated cumulative volume of ice loss in millions of cubic meters from July 2008 through March 2009. Black squares—calculated cumulative ice loss in cubic meters $\times 10^6$. Gray diamonds—heat needed to melt ice in megawatts. B) Gas flux from July 2008 through March 2009 (Werner et al., 2011). Black circles—cumulative gas flux of SO_2 and CO_2 in tonnes since unrest $\times 10^3$. Gray triangles—ratio of SO_2 over $CO_2 \times 10^{-2}$ (SO_2 divided by CO_2 multiplied by 100). C) Earthquakes recorded at instrument "RED" from July 2008 through March 2009 (Dixon and Stihler, 2009; Dixon et al., 2010; Power et al., 2013).

Steam pillars were only seen on exposed rock near the contact with ice and not within a hole in the ice.

On March 20, discrete steam pillars appeared at the base of the exposed 1990 dome, in addition to the usual steam plume of more diffuse origin (Fig. 6E). We do not see evidence of steam pillars earlier in the precursory phase. With a resolution of 90 m pixels, ASTER indicates a heat source but not hot enough to be lava. We do see them in the photographs taken when new dome material is at the surface in 2009. They are also seen in photographs taken in 1990 of the new dome material at the surface with the ice next to the dome. The meaning of the steam pillars is unclear, especially since the visibility of "steam" (really water vapor) depends on atmospheric conditions. However, given their vigor and sudden appearance, we argue that they likely indicate an increase of heat flow in this area. If their appearance was attributable to just atmospheric conditions, we would expect visible changes in other features that otherwise appeared static. No such changes were observed. We suggest that these vigorous features formed as fresh magma moved very close to the surface.

5.2. Features on the East Drift and Crescent glaciers

5.2.1. East Drift glacier

Disruption of the snow and ice mainly occurred on Drift glacier but there was a small amount of disturbance on the East Drift glacier. As early as February 27, ice talus accumulated at the base of the East Drift glacier where it flows into the Drift glacier as noted by an avalanche scarp. What appears to be an ice-rich debris flow occurred on the East Drift glacier sometime between March 25 and 26. The date is constrained by an ASTER image from March 24 that shows nothing on the East Drift glacier, and by observations on March 26 that show disruption and partial removal of ice between the elevation of 2000 and 2600 m. Using Trabant and Hawkins (1997) glacier volumes the removal would be roughly 14.5 M m^3 of snow and ice (Fig. 2). Parts of the East Drift glacier remained intact as seen with crevasses still visible that were blanketed in tephra. The crevasses were prominent particularly at the saddle that connects to the Drift glacier in the summit crater at 2550 m. In addition, on April 4 there is a gully carved in the ice that appears to be less than 100 m wide. This gully most likely formed as water-rich flows were transported down the surface of the glacier.

5.2.2. Crescent glacier

No flows or deposits were observed on the Crescent glacier (Fig. 2). In photographs from March 21, there is a tunnel observed at the basal contact of the glacier and surficial deposits. There were some scour marks photographed on the glacier and the western side of the western cliff that makes the Drift glacier valley in late March, but no deposits were seen in either location. The Crescent glacier area was blanketed in tephra by this time and the windblown products were leaving trails making it more difficult to distinguish debris flows especially if they were ice rich. Also occurring starting in early April was seasonal snow sloughing, which made it more difficult to determine what features were due to eruptive activity.

5.3. Mechanism for melting

Melting ice was caused by a rising body of magma and its exsolving volatiles, causing a rapid increase in the rate of ice loss prior to the eruption starting on March 22 (Fig. 11 and Table 1). A few assumptions on this process are the rising magma loses heat through conduction, and convection carries volatile heat to the glacier base most likely through volatile escape conduits. This causes localized melting of ice and forms glacial cavities, such as ice cauldrons and holes in the ice. We suggest that the volatile escape conduits were clustered in the area of the 1990 dome and the hole in the ice 300 m north of the 1990 dome.

The movement of the glacier has also a role in the melting of the ice. As the glacier moves and blocks of ice calve into the cavities it increases the amount of ice melted. The flow of ice toward the active vent ensured continued melt runoff from the summit crater by moving ice closer to the vent heat source. There was significant disruption of the glacier in the last week before the eruption. This disruption did not form the typical holes in the ice as seen earlier. It formed larger subsidence areas that were irregular in shape. This indicates more widespread and intense gas flux, suggesting that magma was close to the surface at this time.

5.4. Heat flux from body of magma

The energy exchange between magma and the overlying ice can be estimated based on ice melting rates. To date, there are few detailed studies of energy exchange mechanisms of volcano–ice interaction (e.g., Allen, 1980; Höskuldsson and Sparks, 1997; Tuffen et al., 2002; Wilson and Head, 2007). Estimates for heat loss at ice-covered volcanoes in Alaska are limited to the studies done at Mount Wrangell (Benson et al., 2007). However, magmatic heat being released as steam is not accounted for in the ice melting data. The heat loss by steam is not estimated and its relative part in the overall loss of magmatic heat is

unknown. The thermal energy required to melt a given volume of ice is determined by

$$Q = V_i L_i \rho_i$$

where, Q is the heat needed (J/s = watt = 10^{-6} MW); V_i is the rate of ice loss in m^3/s; L_i is the enthalpy of ice (335,000 J/kg); and ρ_i is the density of ice (917 kg/m^3). This equation assumes that all the thermal energy goes into melting ice and is only a minimum. As soon as the ice cavity is open to the atmosphere, an unknown amount of heat is lost to the atmosphere. Therefore, the minimum heat needed to melt the volume of ice is 24 MW in October 2008 and rises to 130 MW in early March. By mid-March the heat needed to melt the ice is 6900 MW (Fig. 11 and Table 1). The melting rate is proportional to the heat output of the body of magma.

5.5. Magma ascent rate

Three lines of investigation provide insight into the magma storage depth prior to the 2009 eruption. First, a small network of continuous GPS receivers recorded both inflation prior to the eruption, and deflation during and after it. The deflation signal, assumed to reflect magmatic withdrawal, is strong enough to constrain magma chamber geometry (Grapenthin et al., 2013), modeled the GPS data and inferred a depressurizing vertical ellipsoid spanning the region from about 18 km to about 6 or 7 km depth. Petrologic studies of erupted products suggest that magma persisted for some time at a depth of about 3.5 to 6 km below the edifice, approximately equivalent to the topmost part of the geodetically-inferred magma chamber (Coombs et al., 2013). Further analysis of melt inclusions could push this deeper, if the magma is found to have been appreciably CO_2-bearing. Finally, hypocenter locations, calculated by DeShon et al. (2007) using a detailed 3D velocity model, shows an aseismic zone from about 7 to 9 km depth.

Using a presumed starting depth of 6 km, based on the analyses described above, we can calculate an average magma ascent rate. Taking a start date of August 1, 2008, coincident with the first observation of abnormal activity, and ending date of March 22, 2009, we arrive at an interval of 233 days. This yields an average ascent rate over the interval of about 25 m/day. Modeling high-quality geodetic data from the 2006 eruption of Augustine volcano, Cervelli et al. (2006) inferred a dike ascent profile directly, resulting in an average ascent rate of about 22 m/day, though the rate of ascent was not linear. In the Augustine case, the dike began to ascend rapidly (c. 100 m/day), but slowed down as it approached the surface.

5.6. Comparing previous eruptive ice loss at Redoubt to 2008–2009

In the past half-century, eruptions in 1966–1968, 1989–1990, and 2009 have removed vast quantities of ice from Redoubt's flanks. All three eruptive episodes were similar, with vents under the upper part of Drift glacier at the breach in the crater rim at about 2400 m ASL, but removed significantly different volumes of ice. By the end of the 2008–09 unrest, ice was partially removed from an elevation of 750 m to 2600 m, and almost completely removed from an elevation of 1500 m to 2600 m, totaling between 100 and 250 M m^3, which is 10–25% of the total volume of the Drift glacier (Waythomas et al., 2012). The 1989–1990 eruption beheaded the Drift glacier, ultimately removing most of the ice between 750 m and 2500 m altitude, amounting to 113–121 M m^3 of snow and ice (Trabant et al., 1994). The 1966–1968 eruptive episode removed about 60 M m^3 of glacier ice between 1500 and 2500 m altitude (Sturm et al., 1986). This establishes the 2008–2009 removal of ice due to unrest as the largest amount of ice loss, up to 2.5 times larger than the 1989–1990 eruption and up to 5 times larger than the 1966–1968 eruptive episode. Although the 2009 eruption ultimately resulted in more ice loss, the destructive power of the lahars seems to be similar to the 1989–1990 eruption. This may be a result of the precursory ice loss releasing debris and water more gradually before the subsequent large scale lahars inundated the Drift River Valley. Would things have been any different if there were no precursory melting? Maybe, the lahar that occurred on March 23 (Waythomas et al., 2012) would have included more ice, if the precursory melting did not occur and all else being equal. Ultimately, months of precursory activity allowed for significant ice loss at a gradual rate. Although major lahar activity has occurred on all flanks of the volcano in Holocene time (Riehle et al., 1981; Begét and Nye, 1994), the last three eruptions have produced large scale lahars only toward the north, in the Drift River valley. During the 1989–1990 eruption, a dark debris flow descended the south side on top of the Crescent glacier (Gardner et al., 1994; Waitt et al., 1994), but this event was miniscule in comparison to lahars in the Crescent River valley 3500 years ago estimated to have a minimum volume of 0.44 km^3 with an error estimate to be an order of magnitude (Riehle et al., 1981; Trabant and Hawkins, 1997). Fig. 2 (asterisk) shows where deposits from this lahar, consisting of several meters of poorly sorted material in two distinct beds, have been exposed by a tributary of the Crescent River.

5.7. Tool to forecast potential eruptive activity

In the past, infrequent airborne observations were the only means available for recording the disruption of glaciers during periods of volcanic unrest. However, because of the increasing availability of high-quality, ortho-rectified, daytime satellite imagery, we can now track changing melt features in great detail, noting both their spatial distribution and evolution over time. Airborne observations also become more efficient and fruitful when the satellite imagery can point the way toward areas of special interest. Tracking melt features, such as holes in ice, ice cauldrons, and ice subsidence, can now facilitate eruption forecasting, because, to first order, the degree of melting scales with the volcanic heat flux. Knowledge of the ice melt rate at a volcano undergoing unrest can thus be very important for predicting its future behavior since the implications of a steadily increasing melt rate are quite different from a constant or declining rate. For example, right before the first major explosion the melt rate reached the highest value (~23 m^3/s) yet seen throughout the precursory unrest. This observation, along with other geophysical and geochemical data, strongly suggested that magma had risen quite close to the surface and that near-term eruption was likely (Fig. 11). Using ice melt rates to forecast future volcanic activity is a method in its infancy. Much works remains to be done to make this a truly quantitative forecasting tool, but, we argue, that the material presented here clearly shows the method's potential utility.

6. Conclusions

Observations of volcano–glacier interactions and ice loss calculations at Redoubt Volcano over the 8-month period of increased thermal activity leading up to the March 2009 eruption provide us with a record of heat flux as a function of time. Melting and collapse of snow and ice formed ice cauldrons, holes in the ice and crevasses, and produced debris flows which left deposits on the north flank of the volcano. The heat source for the melting was a rising body of magma that erupted explosively starting on March 22, 2009. This rising body of magma let off large quantities of superheated volatiles that carried their thermal energy up and out of the edifice, causing a rapid increase in the rate of ice loss prior to the eruption. Evidence for this interpretation comes from the marked correlations among melt rates, gas flux, and episodes of seismicity. The precursory ice loss most likely decreased the volume of subsequent lahars by releasing water at a more gradual pace, ultimately diminishing their destructive potential. The cumulative volume of lost ice over the precursory phase was more than 35 M m^3. This is the first time we have a sufficient quantity and quality of observations to record the ice lost history in such detail, and we suggest that such documentation is a useful tool to forecast potential eruptive activity.

Supplementary data to this article can be found online at http://dx.doi.org/10.1016/j.jvolgeores.2012.10.008.

Acknowledgments

This work supported by the USGS Volcano Science Center. We thank the staff of AVO, in particular, Game McGimsey, Tina Neal, and Kristi Wallace, who made essential observations during overflights. Our colleagues at the Cascade Volcano Observatory, Cynthia Gardner and Mike Doukas, also shared helpful ideas and perspective. Helpful reviews by Joseph Walder and an anonymous reviewer improved the manuscript. We also thank citizens who freely shared their photographs and observations of Redoubt Volcano. Many of our observations were collected during observational overflights over rugged terrain and we thank the capable pilots who made it possible, especially Jerry Morris at Security Aviation who flew the majority of the flights and made sound observations. ASTER data were provided by NASA/GSFC/METI/ERSDAC/JAROS and the U.S./Japan ASTER Science Team. Quickbird imagery is a copyright of DigitalGlobe, Inc. Any use of trade, product, or firm names is for descriptive purposes only and does not imply endorsement by the U.S. government. IKONOS imagery is credited to Worldview.

References

Allen, C.C., 1980. Icelandic subglacial volcanism: thermal and physical studies. Geology 88, 108–117.

Begét, J.E., Nye, C.J., 1994. Postglacial eruption history of Mt. Redoubt, Alaska. Journal of Volcanology and Geothermal Research 62, 31–54.

Benson, C., Motyka, R., McNutt, S., Lüthi, S., Truffer, M., 2007. Glacier–volcano, interactions in the North Crater of Mt Wrangell, Alaska. Annals of Glaciology 45, 48–57.

Björnsson, H., 1975. Subglacial water reservoirs, jökulhlaups and volcanic eruptions. Jökull 25, 1–11.

Björnsson, H., 1988. Hydrology of ice caps in volcanic regions. Vísindafélag Íslendinga, Societa Scientarium Islandica 45, 1–139.

Björnsson, H., Palsson, F., Singurosson, O., Flowers, E., 2003. Surges of glaciers in Iceland. Annals of Glaciology 36, 82–90.

Bull, K.F., Buurman, H., 2013. An overview of the 2009 eruption of Redoubt Volcano, Alaska. Journal of Volcanology and Geothermal Research 259, 2–15.

Buurman, H., West, M.E., Thompson, G., 2013. The seismicity of the 2009 Redoubt eruption. Journal of Volcanology and Geothermal Research 259, 16–30.

Cervelli, P.F., Fournier, T., Freymueller, J., Power, J.A., 2006. Ground deformation associated with the precursory unrest and early phases of the January 2006 eruption of Augustine Volcano, Alaska. Geophysical Research Letters 33 (5 pp.).

Coombs, M.L., Neal, C.A., Wessels, R.L., McGimsey, R.G., 2006. Geothermal disruption of summit glaciers at Mount Spurr Volcano, 2004–6: an unusual manifestation of volcanic unrest. United States Geological Survey Professional Paper 1732-B (33 pp.).

Coombs, M.L., Sisson, T.W., Bleick, H.A., Henton, S.M., Nye, C.J., Payne, A.L., Cameron, C.E., Larsen, J.F., Wallace, K.L., Bull, K.F., 2013. Andesites of the 2009 eruption of Redoubt Volcano, Alaska. Journal of Volcanology and Geothermal Research 259, 349–372.

Cronin, S.J., Neall, V.E., Lecointre, J.A., Palmer, A.S., 1996. Unusual "snow slurry" lahars from Ruapehu volcano, New Zealand, September 1995. Geology 24, 1107–1110.

DeShon, H.R., Thurber, C.H., Rowe, C., 2007. High-precision earthquake location and three-dimensional P wave velocity determination at Redoubt Volcano, Alaska. Journal of Geophysical Research 112 (24 pp.).

Dixon, J.P., Stihler, S.D., 2009. Catalog of earthquake hypocenters at Alaskan volcanoes: January 1 through December 31, 2008. U.S. Geological Survey Data Series, 467 (88 pp.).

Dixon, J.P., Stihler, S.D., Power, J.A., Searcy, C., 2010. Catalog of earthquake hypocenters at Alaskan volcanoes: January 1 through December 31, 2009. U.S. Geological Survey Data Series, 531 (84 pp.).

Fisher, D.A., 1973. Subglacial leakage of Summit Lake, British Columbia, by dye determinations. In: Stelczer, K. (Ed.), Water within Glaciers; Symposium on the Hydrology of Glacier, 95. International Association of Scientific Hydrology Publication, pp. 111–116.

Gardner, C.A., Neal, C.A., Waitt, R.B., Janda, R.J., 1994. Proximal pyroclastic avalanche deposits from the 1989–1990 eruptions of Redoubt Volcano, Alaska — pyroclastic avalanche stratigraphy, distribution, and physical characteristics. In: Miller, T.P., Chouet, B.A. (Eds.), The 1989–1990 Eruption of Redoubt Volcano, AlaskaJournal of Volcanological and Geothermal Research 62, 213–250.

Grapenthin, R., Freymueller, J.T., Kaufman, A.M., 2013. Geodetic observations during the 2009 eruption of Redoubt Volcano, Alaska. Journal of Volcanological and Geothermal Research 259, 115–132.

Gudmundsson, M.T., 2003. Melting of ice by magma–ice–water interactions during subglacial eruptions as an indicator of heat transfer in subaqueous eruptions. Geophysical Monograph 140, 61–72.

Gudmundsson, M.T., Sigmundsson, F., Björnsson, H., 1997. Ice–volcano interaction of the 1996 Gjálp subglacial eruption, Vatnajökull, Iceland. Nature (London) 389 (6654), 954.

Gudmundsson, M.T., Sigmundsson, F., Björnsson, H., Höegnadottir, T., 2004. The 1996 eruption at Gjálp, Vatnajöekull ice cap, Iceland: efficiency of heat transfer, ice deformation and subglacier water pressure. Bulletin of Volcanology 66 (1), 46–65.

Gudmundsson, M.T., Hognadottir, P., Kristinsson, A.B., Gudbjornsson, S., 2007. Geothermal activity in the subglacial Katla caldera, Iceland, 1999–2005, studied with radar altimetry. Annals of Glaciololgy 45, 66–72.

Höskuldsson, Á., Sparks, R.S.J., 1997. Thermodynamics and fluid dynamics of effusive subglacial eruptions. Bulletin of Volcanology 59, 219–230.

Lube, G., Cronin, S.J., Procter, J.N., 2009. Explaining the extreme mobility of volcanic ice-slurry flows, Ruapehu volcano, New Zealand. Geology 37, 15–18.

Miller, T.P., 1994. Dome growth and destruction during the 1989–1990 eruption of Redoubt Volcano. In: Miller, T.P., Chouet, B.A. (Eds.), The 1989–1990 Eruption of Redoubt Volcano, AlaskaJournal of Volcanology and Geothermal Research 62, 197–212.

Nye, J.F., 1976. Water flow in glaciers: jokulhlaups, tunnels and veins. Journal of Glaciology 17 (76), 181–207.

Post, A., Mayo, L.R., 1971. Glacier-dammed lakes and outburst floods in Alaska. U.S. Geological Survery Hydrological Investigations Atlas HA-455, pp. 1–10.

Power, J.A., Stihler, S.D., Chouet, B.A., Haney, M.M., Ketner, D.M., 2013. Seismic observations of Redoubt Volcano, Alaska — 1989–2010 and a conceptual model of the Redoubt magmatic system. Journal of Volcanology and Geothermeral Research 259, 31–44.

Riehle, J.R., Kienle, J., Emmel, K.S., 1981. Lahars in Crescent River valley, lower Cook Inlet, Alaska. Alaska Division of Geological and Geophysical Survey Geologic Report, 53, pp. 1–10.

The 2009 eruption of Redoubt Volcano, Alaska. In: Schaefer, J.R. (Ed.), Alaska Division of Geological and Geophysical Surveys Report of Investigation 2011–2015 (45 pp.).

Schneider, D.J., Hoblitt, R.P., 2013. Doppler weather radar observations of the 2009 eruption of Redoubt Volcano, Alaska. Journal of Volcanology and Geothermeral Research 259, 133–144.

Sisson, T.W., Robinson, J.E., Swinnery, D.A., 2011. Whole-edifice ice volume change A.D. 1970 to 2007/2008 at Mount Rainier, Washington, based on LiDAR surveying. Geology 39 (7), 639–642.

Smellie, J.L., 2002. The 1969 subglacial eruption on Deception Island (Antarctica): events and processes during an eruption beneath a thin glacier and implications for volcanic hazards. In: Smellie, J.L., Chapman, M.G. (Eds.), Volcano–Ice Interactions on Earth and Mars: Geological Society, London, Special Publication, 202, pp. 59–79.

Sturm, M., Benson, C., MacKeith, P., 1986. Effects of the 1966–68 eruption on Mount Redoubt on the flow of Drift glacier, Alaska. Journal of Glaciology 32 (112), 355–362.

Thouret, J.C., Ramírez, C., Gibert-Malengreau, B., Vargas, C.A., Naranjo, J.L., Vandemeulebrouck, J., Valla, F., Funk, M., 2007. Volcano–glacier interactions on composite cones and lahar generation: Nevado del Ruiz, Colombia, case study. Annals of Glaciology 45, 115–127.

Trabant, D.C., Hawkins, D.B., 1997. Glacier ice-volume modeling and glacier volumes on Redoubt Volcano, Alaska. U.S. Geological Survey Water-Resources Investigation Report 97-4187, pp. 1–29.

Trabant, D.C., Waitt, R.B., Major, J.J., 1994. Disruption of Drift glacier and origin of floods during the 1989–90 eruptions of Redoubt Volcano, Alaska. In: Miller, T.P., Chouet, B.A. (Eds.), The 1989–1990 Eruption of Redoubt Volcano, AlaskaJournal of Volcanology and Geothermal Research Special Issue 62 (1–4), 369–385.

Tuffen, H., Pinkerton, H., McGarvie, D.W., Gilbert, J.S., 2002. Melting of the glacier base during a small-volume subglacial rhyolite eruption: evidence from Bla'hnu'kur, Iceland. Sedimentary Geology 149, 183–198.

Waitt, R.B., Gardner, C.A., Pierson, T.C., Major, J.J., Neall, C.A., 1994. Unusual ice diamicts emplaced during the December 15, 1989 eruption of Redoubt Volcano, Alaska. Journal of Volcanology and Geothermeral Research 62, 409–428.

Walder, J.S., Schilling, S.P., Vallance, J.W., LaHusen, R.G., 2008. Effects of lava-dome growth on the Crater Glacier of Mount St. Helens, Washington. In: Sherrod, D.R., Scott, W.E., Stauffer, P.H. (Eds.), A Volcano Rekindled: The Renewed Eruption of Mount St. Helens, 2004–2006United States Geological Survey Professional Paper 1750, 257–276.

Wallace, K.L., Schaefer, J.R., Coombs, M.L., 2013. Character, mass, distribution, and origin of tephra-fall deposits from the 2009 eruption of Redoubt Volcano, Alaska—Highlighting the significance of particle aggregation. Journal of Volcanology and Geothermal Research 259, 145–169.

Waythomas, C.F., Pierson, T.C., Major, J.J., Scott, W.E., 2012. Preliminary observations of voluminous ice-rich and water-rich lahars generated during the 2009 eruption of Redoubt Volcano, Alaska. U.S. Geological Survey Open-File Report 2012-1078, 42.

Werner, C., Kelly, P.J., Doukas, M., Lopez, T., Pfeffer, M., McGimsey, R., Neal, C., 2013. Degassing of CO_2, SO_2, and H_2S associated with the 2009 eruption of Redoubt Volcano, Alaska. Journal of Volcanology and Geothermal Research 259, 270–284.

Werner, C., Evans, T., Kelly, P.J., McGimsey, R.G., Pfeffer, M.P., Doukas, M., Neal, C.A., 2011. Deep magmatic degassing vs. scrubbing: elevated CO_2 emission and C/S in the lead-up to the 2009 eruption of Redoubt Volcano, Alaska. Geochemisty Geophysics Geosystems 13 (3) (18 pp.).

Wessels, R.L., Vaughan, R.G., Patrick, M.R., Coombs, M.L., 2013. High-resolution satellite and airborne thermal infrared imaging of precursory unrest and 2009 eruption at Redoubt Volcano, Alaska. Journal of Volcanology and Geothermeral Research 259, 248–269.

Wilson, L., Head, J.W., 2007. Heat transfer in volcano–ice interactions on Earth. Annals of Glaciology 45, 83–86.

Yount, M.E., Miller, T.P., Emanuel, R.P., Wilson, F.H., 1985. Eruption in an ice-filled caldera, Mount Veniaminof, Alaska Peninsula. In: Bartsch-Winkler, S., Reed, K.M. (Eds.), The United States Geological Survey in Alaska: Accomplishments During 1983: U.S. Geological Survey Circular, C0945, pp. 58–60.